RESEARCH PAPER | Engineering | Volume : 3 | Issue : 5 | May 2013 | ISSN - 2249-555X

Single Phase Dual Full Bridge Bi-directional DC-DC Converter for High power applications

KEYWORDS: Bi-directional dc-dc converter, galvanic isolation, loss analysis, charger,dis-charger, EDLC

P. Divya Sri
M.Tech Student, Dept. of Electrical & Electronics Engg, KL University, A.P., India

Dr. P. Hari Krishna Prasad
Professor, Dept. of Electrical & Electronics Engg, KL University, A.P., India

ABSTRACT *This paper presents a bi-directional dc-dc converter for use in high powerapplications implementing dual operation of full bridge dc-dc converter. The proposed topology has two single phase full bridge converters on either side of the isolation transformer considering EDLC as energy storage device. Typical applications of this scheme are auxiliary power supply in fuel cell vehicles and battery charging/dis-charging systems providing high efficiency, high power density and galvanic isolation. The overall efficiency from dc input to dc output terminals is accurately measured and loss analysis is carried out to estimate effectiveness of power switching devices. Moreover, the dc-dc converter can charge the capacitor bank from zero to rated voltage without any external pre-charging circuit.*

I. INTRODUCTION

Generally, electric power generated by renewable energysources is unstable in nature, thus producing a bad effecton the utility grid. This fact spurs research on energy storagesystems to smooth out active-power flow on the utility grid. Fig. 1 shows a simplified existing energy storage systememploying a line-frequency (50- or 60-Hz) transformer, a PWMconverter, a bidirectional chopper, and an energy storage devicesuch as electric double layer capacitors (EDLCs) or lithium-ionbatteries. The transformer is indispensable for some applicationsthat require voltage matching and/or galvanic isolation betweenthe utility grid and the energy storage device. Replacingthe line-frequency transformer with a high-frequency isolateddc-dc converter would make the energy storage system morecompact and flexible.

Various bidirectional isolated dc-dc converters have been proposedas the interface to energy storage devices with focus onautomotive or fuel cell applications. Most of the presented dc-dcconverters have asymmetrical circuit configurations to couplethe two dc links having largely different voltages, several tensvolts and several hundred volts.

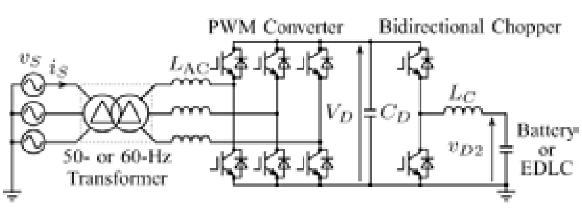

Fig.1. Existing energy storage system employing a 50- or 60-Hz transformerfor voltage matching and/or galvanic isolation.

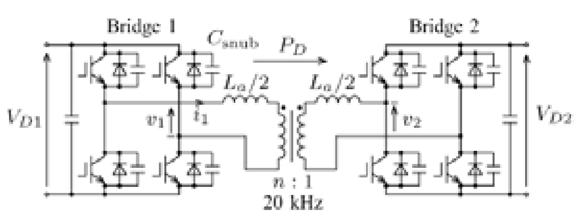

Fig.2. Bidirectional isolated dc-dc converter.

Fig.2 depicts a bidirectional isolated dc-dc converter presented in 1991. It had two symmetrical single-phasevoltage-source full-bridge converters. It suffered from a lowefficiency because the first-generation IGBTs were used asswitching power devices at that time. However, advancementin power device technology over the last decade hasenabled the dc-dc converter to operate at an efficiency as highas 97% by using the latest trench-gate IGBTs.In addition, the use of silicon-carbide power devices in the nearfuture will raise it to 99%. Therefore, the dc-dc converter inFig. 2 has become a promising candidate as a power electronicinterface for an energy storage system. A bidirectional converterhas been discussed to exchange electric power betweena fuel cell, a battery, and a load.

Fig.3 shows the energy storage system using the bidirectionalisolated dc-dc converter in Fig.2. Appropriately choosingthe transformer turn ratio enables to design the voltage ratingof the energy storage device, independent of the utility voltage.The energy storage device is directly connected to one of the dclinks of the dc-dc converter without any chopper circuit. Nevertheless,the dc-dc converter continues operating even when thevoltage across the energy storage device, v_{D2}drops along withits discharge.

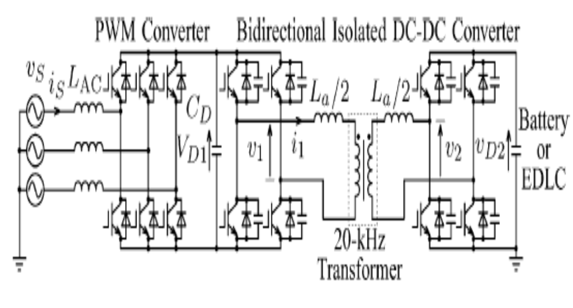

Fig. 3. Alternative energy storage system based on the bidirectional isolateddc-dc converter.

However, no paper has addressed the permissible voltagerange of in terms of power loss and peak-current, andno experimental verification has been confirmed, concerningFig.3. This paper analyzes the relationships between the powerloss, the peak current, and v_{D2}in a dc-dc converter rated at10 kW and 20 kHz with V_{D1}fixed at 320 V.Then, the dc-dcconverter is designed, constructed, and tested to verify theanalysis. A 2.6-kJ energy storage system using an electrolyticcapacitor bank, together with the dc-dc converter, demonstratesstable charging and discharging operation. Besides, the dc-dconverter can charge the capacitor bank from zero to the ratedvoltage without any external pre-charging or starting-up circuit.

Volume : 3 | Issue : 5 | May 2013 | ISSN - 2249-555X

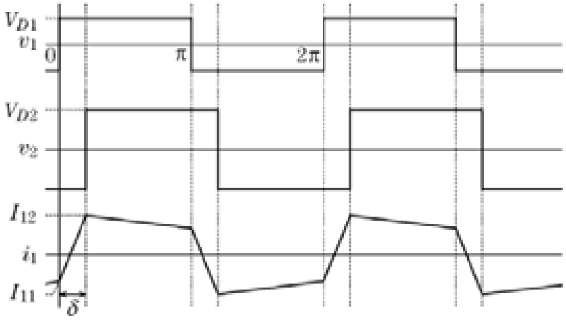

Fig. 4. Simplified theoreticalwaveforms used to analyze the power losses whenV_{D1}<V_{D2}

II. THE BIDIRECTIONAL ISOLATED DC–DC CONVERTER

A. Operation Principle and Simplified Theoretical Waveforms

Fig.4 illustrates simplified theoretical waveforms of thedc-dc converter where $V_{D1}<V_{D2}$. The two single-phasevoltage-source full-bridge converters produce square voltages $v_1$and v_2. The power transfer $P_D$can simply be controlled byadjusting the phase shift between $v_1$and v_2,δis expressed by

$$P_D = \frac{V_{D1}V_{D2}}{\omega L}\left(\delta - \frac{\delta^2}{\pi}\right)$$

Wherew(=2∏f) is the switching angular frequency of the two-single-phase voltage-source full-bridge converters, and L is thesum of the transformer leakage inductance $L_{trans}$and that of theauxiliary inductors L_a.

As shown in Fig. 4, this paper defines a set of two instantaneousvalues of the current $i_1$as "switching currents," I_{11}andI-$_{12}$which are calculated as

$$I_{11} = -\frac{(V_{D1}+V_{D2})\delta + (V_{D1}-V_{D2})(\pi-\delta)}{2\omega L}$$

and

$$I_{12} = \frac{(V_{D1}+V_{D2})\delta - (V_{D1}-V_{D2})(\pi-\delta)}{2\omega L}$$

$I_{11}$and I_{12} are the instantaneous values of $i_1$when $v_1$and v_2,respectively, change its polarity from negative to positive.

This paper refers a single-phase voltage-source full-bridge-converter as a "bridge." In the following experiments, the transformerturn ratio is unity (n=1) for the sake of simplicity.

TABLE I
CIRCUIT PARAMETERS OF THE DC-DC CONVERTER

Rated power		10 kW
Rated DC voltage	V_{D1}, V_{D2}	360 V
DC capacitor	C_D	7,100 µF
Unit capacitance constant	H	46 ms
Transformer core material		Finemet FT-3M
Transformer turn ratio	n	1 : 1
Transformer leakage inductance	L_{trans}	1.6 µH (1.6%)
Transformer winding resistance	R_{trans}	17 mΩ (0.13%)
Auxiliary inductor	$L_a/2$	20 µH (19%)
Auxiliary inductor core material		Ferrite (PC44)
Inductor winding resistance	$R_a/2$	20 mΩ (0.15%)
Snubber Capacitor	C_{snub}	0.01 µF (1.6%)
Switching Frequency	f	20 kHz

B. Experimental Circuit of the DC–DC Converter

Table I summarizes the circuit parameters of the dc-dc converter.Four auxiliary inductors, totally having L_a = 40 µH,are connected in series with the transformer to obtain an inductanceof L = 41.6 µH together with the leakage inductance ofthe transformer,L_{trans}(= 1.6µH). The inductance of 41.6µH is sufficient to maintain a control resolution of power transferaround 120 W because a time resolution of the controller operatedat 20 MHz is 50 ns, corresponding to 0.36^0 at 20 kHz.

The following sections analyze relationships between powertransfer and power losses in the dc-dc converter. The powerlosses depend not only on the power transfer, but also the dcvoltage V_{D2}. When V_{D2}drops along with discharge of theenergy storage device, power loss increases at a given powertransfer.

III. SNUBBER LOSS

A. Operating Points and ZVS Conditions

In Fig.2, a snubber capacitorC_{snub} is connected in parallelwith each IGBT both to reduce switching loss and to damp outovervoltage. If the IGBT is turned on with its snubber capacitorcharged, the IGBT shorts out the snubber capacitor and dissipatesthe energy stored in the capacitor. This paper refers to thispower loss as "snubber loss."

Each IGBT can be turned on in zero-voltage switching (ZVS) manner to generate no snubber loss when both dc voltages areequal ($V_{D1} = V_{D2}$), and the power transfer is sufficient to ensurethe ZVS operation. However, when $V_{D1} \neq V_{D2,}$ the IGBTis not necessarily turned on in ZVS manner.

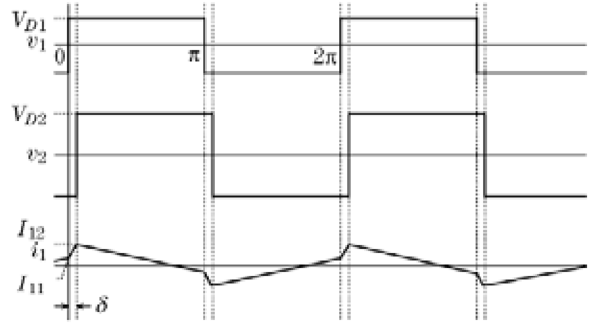

Fig. 5. Waveforms when a positive I forces bridge 1 to operate in hardswitchingmanner.

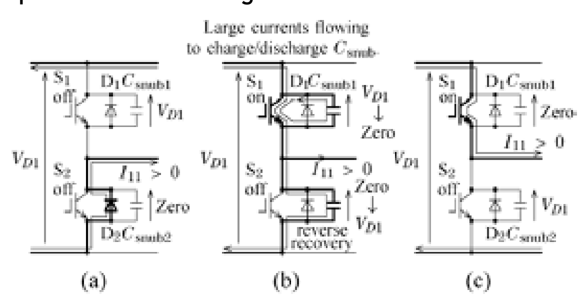

Fig. 6. Hard switching on a leg in Bridge 1: (a) just before the dead time ends,(b) rapid charging/discharging of C_{snub1} , and Csnub$_2$, (c) after commutation.

Fig.5 shows simplified theoretical waveforms when theIGBTs in bridge 1 are turned on in hard-switching manner.The power transfer is less than that in Fig. 4 although the dcvoltages $V_{D1}$and $V_{D2}$are the same as those in Fig.4. Theso-called "reverse recovery" occurs in the free-wheeling diodesin bridge 1 because the switching current $I_{11}$is positive as canbe seen in Fig. 5. However, the four IGBTs in bridge 2 areturned on in ZVS manner. One can classify the turn-on processesof the

Volume : 3 | Issue : 5 | May 2013 | ISSN - 2249-555X

IGBTs in bridges 1 and 2 into the following three:1) hard switching operation; 2) incomplete ZVS operation;and 3) ZVS operation, depending on the power transfer P_D,the phase shift δ, the dc voltages $V_{D1}$and V_{D2}, and the deadtime. The hard-switching operation and the incomplete ZVSoperation can take place only in one bridge, whose dc voltage islower than the other. The following calculations mainly focuson phenomena in bridge 1 because those in bridge 2 can be-described alike.

B. Calculations of the Snubber Loss

1) Hard-Switching Operation: Fig.6 shows circuit modeswhen a leg (for example, consisting of $S_1$and S_2) operates inhard-switching manner. The IGBTs in bridge 1 are turned on inhard-switching manner if the dc voltage $V_{D1}$is lower than V_{D2},and the following equation is satisfied:

$$\delta \le \frac{V_{D2} - V_{D1}}{2V_{D2}}\pi$$

The snubber capacitor ofS_1 , or C_{snub1}, has been charged at[see Fig. 6(a)] before the end of the dead time. Just after-$S_1$is turned on, D_2experiences reverse recovery.C_{snub1}Dis-chargesfrom $V_{D1}$to zero while C_{snub2}charges from zero to V_{D1}[see Fig. 6(b)]. Only an equivalent resistance of S_1limitsthe charging/discharging currents, resulting in a joule loss of$W_{snub} = C_{snub}V_{D1}^2$. Note that W_{snub}represents an amount ofenergy lost at one switching per leg where$C_{snub1} = C_{snub2} = C_{snub}$. Then, the snubber loss P_{snub1}in bridge 1 is calculatedas

$$P_{\mathrm{snub1}} = 4W_{\mathrm{snub1}}f = 4C_{\mathrm{snub}}V_{D1}^2 f.$$

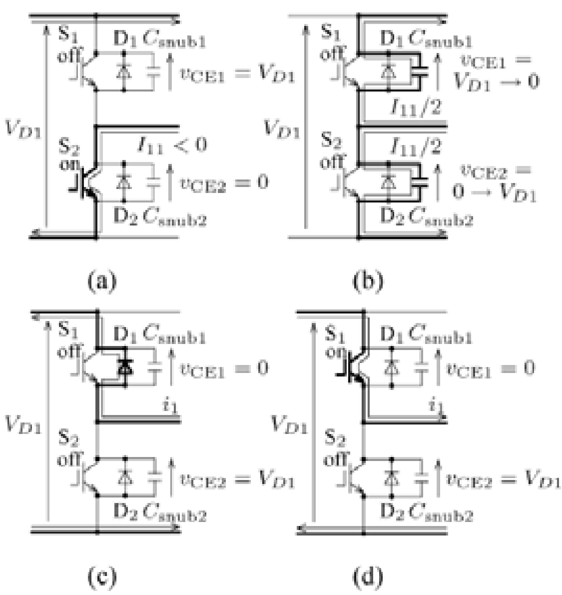

Fig. 7. ZVS on a leg in Bridge 1: (a) just before the dead time starts, (b) just after the dead time starts, (c) diode free wheeling, and (d) current polarity alternates after the dead time.

2) ZVS Operation: Fig.7 shows circuit modes when a legin bridge 1 operates in ZVS manner. Before the dead time, thecurrent of $I_{11}$is flowing in S_2[see Fig. 7(a)]. Turning off-S_2starts the dead time. The current flowing in $S_2$is commutated to$C_{snub1}$and C_{snub2}. A resonance begins between the inductanceL(see Fig. 2), C_{snub1}, and C_{snub2}. C_{snub1}discharges from$V_{D1}$to zero while C_{snub2} charges from zero to V_{D1}. OnceC_{snub1}discharges down to zero, the current is commutated to D_1 [seeFig. 7(c)]. Providing a gating signal during conduction ofD_1makes S_1ready to conduct the current. S_1actually starts to conductthe current in ZVS manner after the current in decaysto zero and alternates its polarity [see Fig. 7(d)]. This operationresults in no snubber loss.

3) Incomplete ZVS Operation: The IGBTs in bridge 1can not necessarily be turned on in ZVS manner even if theswitching current $I_{11}$is negative. Unlike in the ZVS operation,C_{snub1}does not discharge down to zero, and C_{snub2} does notcharge up to V_{D1}, if the magnitude of I_{11}, or $|I_{11}|$ is smallerthan I_{min}, where

$$I_{\min} = \frac{2\sqrt{V_{D1}V_{D2}}}{Z_r}$$

and

$$Z_r = \sqrt{\frac{L}{C_{\mathrm{snub}}}}$$

In this case, the operation of the leg makes adirect transition from Fig.7(b) to (d), not through (c). Turningon $S_1$with the charged snubber capacitor C_{snub1}results in anamount of snubber loss. This paper refers to this as "incompleteZVS operation."

The following is the calculation of the snubber loss caused bythe incomplete ZVS operation. The collector-emitter voltage ofS_1,v_{CE1} in Fig. 7(b) can be expressed as

$$v_{\mathrm{CE1}}(t) = \frac{(V_{D1}+V_{D2}) + (V_{D1}-V_{D2})\cos\omega_r t}{2} - \frac{Z_r|I_{11}|\sin\omega_r t}{2}$$

wheretis the time after the dead time starts, and$w_r(=1/\sqrt{LC_{snub}})$ is the resonant angular frequency of C_{snub}andL. The collector-emitter voltage $v_{CE1}(t)$ is not zero at the endof the dead time. As a result, the IGBT dissipates anenergy of $W_{snub1} = C_{snub}$when it is turned on.Therefore, the snubber loss P_{snub1}in bridge 1 is calculated as

$$P_{\mathrm{snub1}} = 4fC_{\mathrm{snub}}\{v_{\mathrm{CE1}}(T_d)\}^2$$

s can be seen in (5) and (9), the snubber loss is proportionalto the capacitance of the snubber capacitors. Minimizingthe parasitic inductance leads to the use of small snubber capacitorswithout an excessive overvoltage appearing across anIGBT, thus resulting in reducing the snubber loss.

IV. PROFILE OF THE CURRENT AND RELATED LOSSES

A. Conducting Loss in the IGBTs

This paper approximates both the on-state voltage across theIGBT,$V_{CE(sat)}$, and the forward voltage drop across the freewheelingdiode,V_F , to be 1.5V, that is,$V_{CE(sat)} = V_F = 1.5V$,independent of the current flowing in them. The conductingloss in the IGBTs and diodes, P_{cond}can be calculated from theaverage of the absolute value of the current i_1.When either bridge 1 or bridge 2 is operated in hard-switchingmanner, calculation on Fig. 5 yields:

$$\langle|i_1|\rangle = \frac{1}{\omega L}\left\{\frac{V_{D1}V_{D2}}{|V_{D1}-V_{D2}|}\frac{\delta^2}{\pi} + |V_{D1}-V_{D2}|\frac{\pi}{4}\right\}$$

On the other hand, when both bridge 1 and bridge 2 are operatedin either ZVS or incomplete ZVS manner,$<|i_1|>$can be calculatedfrom Fig. 4:

$$\langle|i_1|\rangle = \frac{V_{D1}V_{D2}}{\omega L(V_{D1}+V_{D2})}\left\{-\frac{\delta^2}{\pi} + 2\delta + \frac{(V_{D1}-V_{D2})^2}{V_{D1}V_{D2}}\frac{\pi}{4}\right\}$$

Both $I_{11}$and I_{12}have to be obtained first to calculate $<|i_1|>$,and then either (10) or (11) should be applied, depending on theswitching manner.

B. Copper Loss in the Transformer and the Auxiliary Inductors

Calculation on the waveforms in Figs. 4 and 5 yields the rmsvalue of i_1, orI_1.

Volume : 3 | Issue : 5 | May 2013 | ISSN - 2249-555X

$$I_1 = \frac{\sqrt{V_{D1}V_{D2}}}{\omega L}\sqrt{-\frac{4}{3\pi}\delta^3 + \delta^2 + \frac{\pi^2}{12}\frac{(V_{D1}-V_{D2})^2}{V_{D1}V_{D2}}}$$

regardless of the switching manner. The copper loss in the transformerand the inductors,P_{copp}, is obtained as

$$P_{\rm copp} = (R_{\rm trans} + R_a)\cdot I_1^2$$

whereR_{trans} (=17mΩ) is the winding resistance of the transformer,and R_a (=40mΩ) is that of the auxiliary inductors.

C. Core Loss in the Auxiliary Inductors

The four auxiliary inductors were constructed using ferrite(TDK PC44) cores. The effective cross-sectional area of eachcore wasA_e =328 mm^2 , the effective volume wasV_e =37.2 cm^3, and the turn number wasN. An air gap ofwas introduced in the magnetic path. Thus, theinstantaneous magnetic flux density is approximately expressedas

$b_{ind} = \mu_0/g\ Ni_1$

where$\mu_0$is the permeability of vacuum. The datasheet ofPC44 indicates that its core loss per volume is600kW/m^{3}when the maximum flux density is 200 mT at afrequency of 100 kHz at a temperature of 25^{0}C.

In a power electronic context, the Steinmetz equationhelps well to calculate an amount ofcore loss in a magnetic material where k is a material constant, fis a frequency of magnetization, and B is the maximum fluxdensity. The exponents, α andβ, are not constant values, butdepend on f, B, and the waveform of the magnetic flux. Whena ferrite core is excited at 20 kHz, the eddy-current loss can bemuch smaller than the hysteresis loss. Thus, αis assumed tobe unity. The other exponent βusually ranges from 2.6 to 2.8.However, this paper takes an approximation of β=2 so as tokeep the analysis simple. This approximation allows to treat thecore loss in the same way as the copper loss.

If the core loss per volume in PC44 can be approximatedby mfB^2, the coefficient m is given as 0.15 mW/HzT^2. Thispaper assumes that a sinusoidal 20-kHz current having an rmsvalue as large as $I_1$is responsible for the core loss in the auxiliaryinductors. The core loss in the four auxiliary inductors canbe calculated as

$$P_{\rm core}[{\rm W}] = 4mf\left(\frac{\mu_0}{g}N\sqrt{2}I_1\right)^2 V_e = \frac{8mf\mu_0^2N^2V_e}{g^2}I_1^2$$

where√2 is the coefficient to transform an rms value into anamplitude. Therefore, the core loss in the four auxiliary inductorscan be treated as an equivalent winding resistance of

$$R_{\rm core(ind)} = \frac{8mf\mu_0^2N^2V_e}{g^2} = 23\ {\rm m\Omega}$$

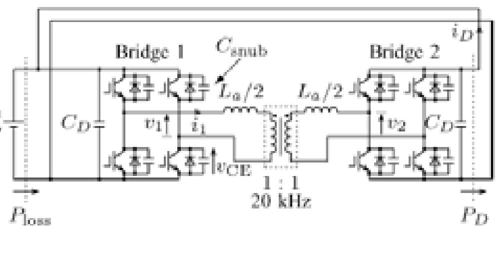

Fig 8.Experimental circuit to measure the power loss of the dc-dc converter.

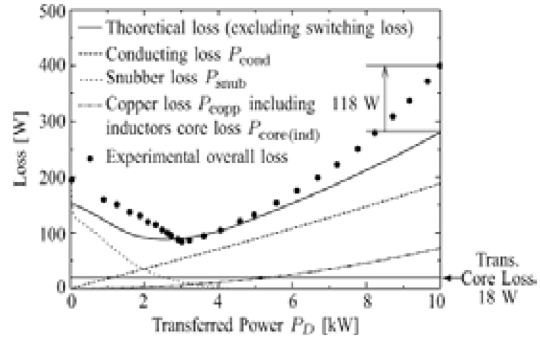

Fig 9. Comparison between calculated and experimental power losses atV_{D1} = V_{D2}= 350 V.

This equivalent resistance enables to calculate the core lossin the auxiliary inductors as a part of copper loss. Further detailedanalysis, should bring animprovement of accuracy to the core-loss calculation althoughit is out of the scope of this paper.

V. POWER LOSSES AND LOWER LIMIT OF V_{D2}

A. Comparison Between Theoretical and Experimental Losses

Theoretical losses described in the previous section are comparedto measured results on the basis of an experimental dc-dcconverter rated at 10 kW and 20 kHz. Fig.8 shows the experimentalcircuit to measure the overall loss of the dc-dc converter.The circuit parameters in Fig.8 are the same as those in Table I.Both theoretical calculation and experimental measurement arecarried out under V_{D1} = V_{D2} =350 V.

Note that in Fig.8 is a dc voltage source. A connectionbetween the two dc links allows the power $P_D$to be regeneratedback to the dc voltage source. Thus, the power coming from $V_D$equals P_{loss}, that is the overall loss in the dc-dc converter.

Fig. 9 shows comparisons between the theoretical and experimentallosses. The solid line corresponds to the theoreticaloverall loss P_{theory}, although it excludes the switching loss inthe IGBTs. Even in the ZVS operation, the switchingloss is not zero due to the so-called "tail current" in the IGBTs. Itrequires modeling of the IGBT switching behavior in this dc-dcconverter to theoretically predict the switching lossP_{sw}. However,it is beyond the scope of this paper.

When P_D = 10kW, the theoretical losses were obtained asfollows. The conducting loss was P_{cond} =189 W. The snubberloss was P_{snub} = 0 W. The copper loss both in the transformerand the inductors P_{copp} = 73 W including the core loss inthe inductors,$_{Pcore(ind)}$. The core loss in the transformer was$_{Pcore(tr)}$ = 18 W, almost independent of the power transfer.Thus, the theoretical overall loss is 282 W.

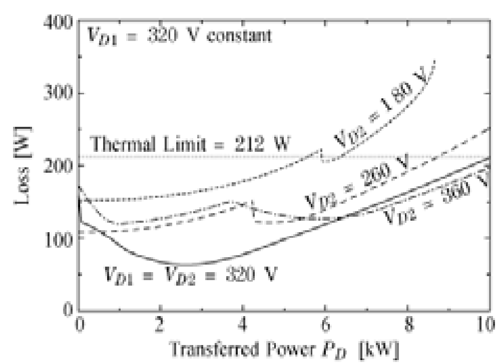

Fig 10. Sum of theoretical conducting and snubber losses (P + P) when P is positive.

Volume : 3 | Issue : 5 | May 2013 | ISSN - 2249-555X

The experimental results,P_{loss}, on the other hand, was400 W. Thus, the difference between the theoretical and measuredresults were 118 W. It would include the switching lossin the IGBTs that was excluded from the theoretical overall loss. Although the difference of118W– 90 W = 28 W can't be identified, the theoreticalcalculations can be valid because the error of 28Wbcorrespondsto 0.28% of the power transfer of 10 kW, and 7% of the measuredoverall loss of 400 W.

A 250-V, 5-kW bidirectional isolated dc-dc converter was constructed and tested in . The dc-dc converter employedthe third-generation planar-gate IGBTs rated at 600 V and100 A. The overall loss of the dc-dc converter was measuredat six switching frequencies from 10 to 20 kHz with a step of2 kHz. This measurement enabled to extract the switching lossfrom the overall loss because the switching loss is proportionalto the switching frequency. As a result, the switching losswas approximately 75 W at a power transfer of 5 kW and aswitching frequency of 20 kHz. The switching loss of 90 Win the 350-V, 10-kW dc-dc converter in this paper can be areasonable value, considering the raised voltage from 250 V to350 V, the increased power from 5 to 10 kW, and the use of thelatest trench-gate IGBTs.

B. Thermal Limit and V_{D2}

Fig. 10 shows calculated results of conducting and snubberlosses in the IGBTs when the power transferis positive. Once dc voltage was kept constant at 320V, whilethe other dc voltage was changed as a parameter. Achievingthe ZVS operation becomes difficult with $V_{D1} \neq V_{D2}$, comparedto $V_{D1}=V_{D2}$= 320 V, resulting in an increased snubberloss around P_D = 3 kW.

Fig. 10 defines $P_{cond} + P_{snub}$ = 212 W at$V_{D1} = V_{D2}$as a "thermal limit." The losses in the IGBTs, whichare the most dominant in the overall loss, may make the IGBTmodules mounted on a heatsink suffer from the highest temperature.The temperature of the IGBT modules, more precisely thesemiconductor chips in the modules, determines the maximumpower transfer. Therefore, this paper considers only the lossesin the IGBT modules as the thermal limit.

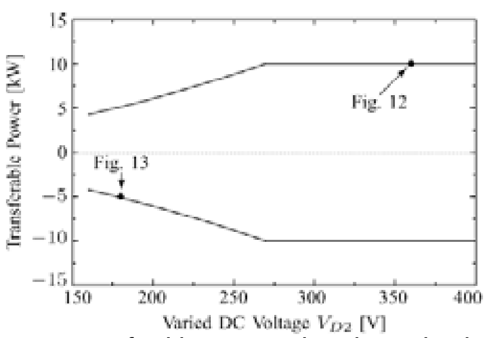

Fig. 11. Transferable powers when the peak value of current i_1 is limited to 60A, and two operating points in experiments.

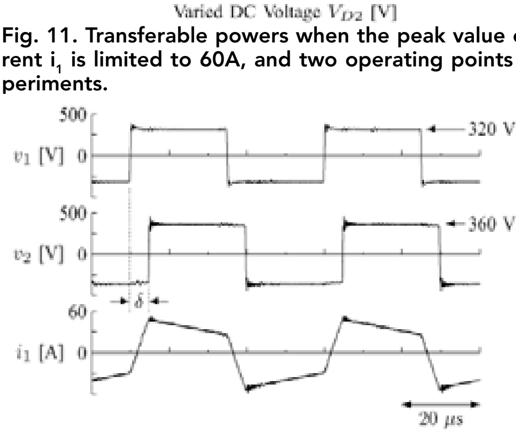

Fig. 12. Experimental waveforms when V_{D1} = 320V, V_{D2} = 360 V, δ =35⁰ , and P_D = 10 kW.

WhenV_{D2} = 180V , the losses in the IGBTs exceed thethermal limit at P_D> 5.6 kW. Hence, when V_{D2} = 180V,the dc-dc converter has to operate under 5.6 kW. WhenV_{D2} = 260V, the losses in the IGBTs exceed the thermal limit atP_D> 8.6 kW. Likewise, the dc voltageimposes limitations on maximum power transfer.

VI. PEAK CURRENT IN THE AUXILIARY INDUCTORS

The ferrite cores in the auxiliary inductors would be magneticallysaturated if the current $i_1$exceeds 60 A because themagnetic flux density reaches 0.3 T as calculated by (14). Thedc-dc converter has to be operated considering the limitation onthe peak value of i_1. The peak current imposes limitationson the dc voltage V_{D2}. When $V_{D1} > V_{D2}$, the peak currentI_{1peak}equals I_{11}. When $V_{D1} < V_{D2}$, the peak currentI_{1Peak}equals I_{12}.

Fig.11 shows maximum power transfer when the peak currentis limited lower than 60 A. Solid dots "•" indicate the operatingpoints of the waveforms shown in Figs. 12 and 13. WhenV_{D2} = 180 V, I_{1peak} exceeds 60 A at P_D = 5.1kW. WhenV_{D2} = 260 V, I_{1peak} exceeds 60 A at P_D= 9.4 kW. Both thepower loss and the peak current impose limitations on the powertransfer P_D and the dc voltage V_{D2}. Operation of the dc-dc converterhas to satisfy both limitations.

Fig. 12 shows the observed waveforms when one dc voltageis 320V while the other is 360V at P_D = 10kW from bridges 1to 2. Fig. 13 shows another example of the observed waveformswhich was taken when V_{D1} = 320 V while V_{D2} = 180 V at P_D = 5kW from bridges 2 to 1. The power transfer$P_D$waslimited below 5 kW, as shown in Fig. 11 when the dc-dc converterhad a set of dc voltages of V_{D1} = 320 V andV_{D2} = 180 V. The peak current $I_{peak}$was 60 A in Fig. 13, as calculatedin this section.

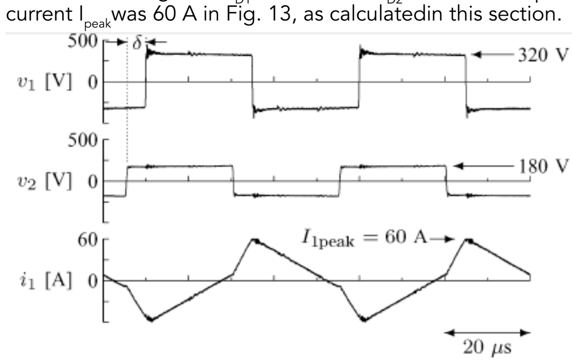

Fig. 13 Experimental waveforms when V_{D1} = 320 V, V_{D2} = 180 V, δ= -41⁰ , and P_D = -5 kW.

VII. APPLICATION TO AN ENERGY STORAGE SYSTEM

A. The 200-V, 10-kW, 2.6-kJ Laboratory Model:

Fig.14 depicts the experimental energy storage system ratedat 200 V, 10 kW, and 2.6 kJ. Circuit parameters in the dc-dcconverter were the same as those in Table I. An electrolytic capacitorbank of 60,000μF was used to simulate an EDLCbank. The capacitor bank is charged up to 350 V and dischargeddown to 190 V. Thus, an energy of 2.6 kJ is stored into, and releasedout of, the capacitor bank. It corresponds to 70% of theenergy stored in C_{ES}at v_{D2} = 350 V. The carrier frequency ofthe PWM converter used as the front end was 10 kHz.

B. Charging and Discharging of the Capacitor Bank

Fig.15 shows the observed waveforms when the energystorage capacitor bank $C_{ES}$was repetitively charged up to350 V, and then discharged down to 190 V. The waveform ofwas observed via a low-pass filter with a cut-off frequencyof 800 Hz. The maximal power transfer was 9.3 kW. In thisexperiment, the phase shift had a square waveform with anamplitude of 30⁰to make the controller simple. In actual energystorage systems, however, the power transfer P_D should begiven by power demand, or a higher level controller regulatingthe voltage on the utility grid.

VIII. STARTING PROCEDURE

At the starting of the system, an inrush current wouldflow into the auxiliary inductors $L_a$and the transformer ifbridge 1 produced a square voltage of $v_1$atv_{D1} = 320 V and v_{D2} = 0V. The inrush current would result in magneticsaturation in the cores of L_a, leading to an even larger inrushcurrent. Hence, this paper presents a special operation modecalled "pre-charging operation" to charge the capacitor bankfrom zero to the rated voltage of 320 V, preventing such aninrush current from flowing. The pre-charging operation allowsthe energy storage system to require no external starting-up orpre-charging circuit. The pre-charging operation presented in thispaper can be considered as a well-known "soft-start" procedureof dc-dc converters. However,experimental verification of the pre-charging operation makes a technical contribution to theenergy storage system with the large dc capacitor bank.

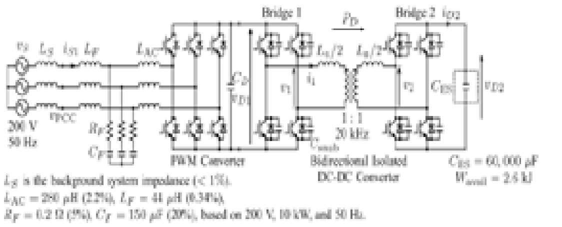

Fig.14. A 200 V, 10kW experimental circuit with energy-storage electrolytic capacitors of 60 000μF to simulate an EDLC bank.

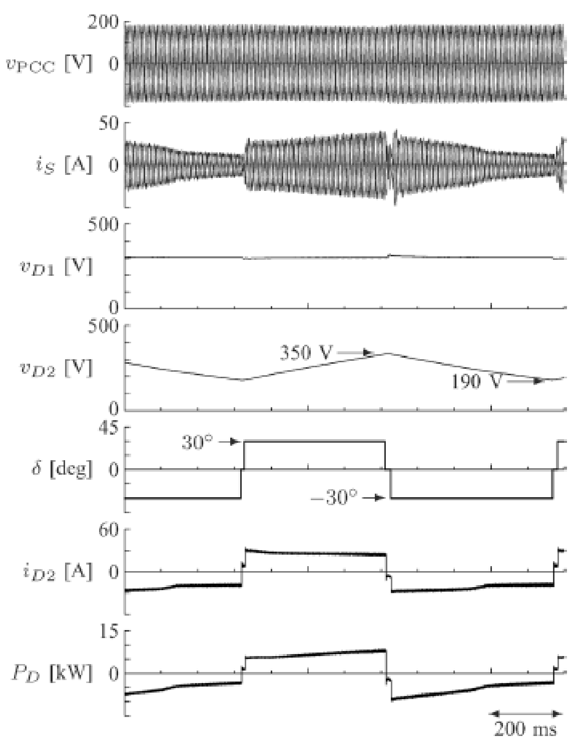

Fig.15. Experimental waveforms of charging and discharging of the capacitorbank (Wavail = 2:6 kJ).

Fig.16 shows the starting-up and pre-charging transient waveformsof the dc-dc converter when the capacitor bank beganbeing charged from 0 to 320 V. In this experiment, v_{D2}hadbeen already charged up to 320 V before the dc-dc converterstarted the pre-charging operation. Bridge 1 produced a voltage$v_1$with a duty ratio of rather than 100% while bridge2 was operated as a diode rectifier with all the IGBTs kept off.The first pulse of had a half duty ratio of d/2 = 10% to suppressdc magnetization of the transformer. The peak value ofat the first pulse of v_1, I_{1pp} is expressed as

$$I_{1pp} = \frac{\pi V_{D1}}{\omega L}\frac{d}{2}$$

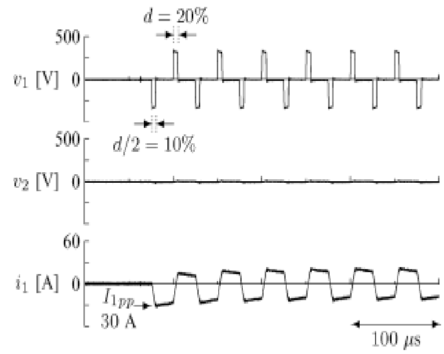

Fig.16. Transient waveforms when the dc-dc converter starts pre-charging thecapacitor bank.

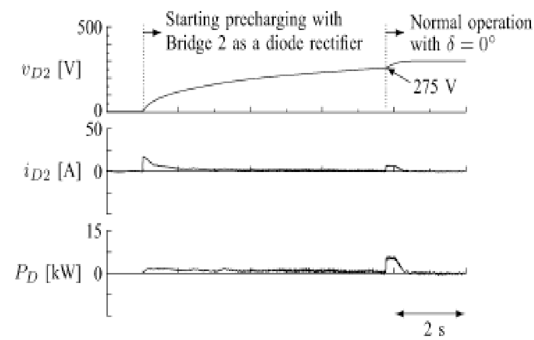

Fig.17. Experimental waveforms of dc voltage, current, and power in thepre-charging period.

The negative peak current reached 30 A in Fig. 16 while itstheoretical value was 19.2 A.Fig. 17 shows the experimental waveforms of the dc voltage,current, and power. The starting procedure took approximately8 s to charge the capacitor bank from zero to 320 V. No excessiveinrush current flowed into the capacitor bank. When thevoltage across the capacitor bank, v_{D2}reached 275 V, the dc-dcconverter changed its operation mode from the pre-charging operationto the normal operation with the square voltages of$v_1$and $v_2$having no phase shift (d = 100% and δ = 00). Thepower transfer $P_D$in the normal operation at δ has anegative-feedback effect to balance the two dc voltages$v_{D1}$and v_{D2}due to the existence of the dead time. Therefore,$v_{D2}$was charged up to the same voltage as v_{D1}naturally afterv_{D2}reached 275 V.

IX. CONCLUSION

This paper has addressed a bidirectional isolated dc-dcconverter suitable for an energy storage system. Theoreticalcalculations of power losses and peak current have clarified thedc-voltage limitations in the energy storage system. Experimental results have revealed that the dc-dc converter can chargeand discharge the capacitor bank properly. Moreover, the dc-dcconverter can charge the capacitor bank from zero to the ratedvoltage without any external pre-charging circuit.

REFERENCE [1] P. F. Ribeiro, B. K. Johnson, M. L. Crow, A. Arsoy, and Y. Liu, "Energystorage systems for advanced power applications,,"Proc. IEEE,vol. 89, no. 12, pp. 1744–1756, Dec. 2001. | [2] T. Kinjo, T. Senjyu, N. Urasaki, and H. Fujita, "Output levelling ofrenewable energy by electric double layer capacitor applied for energystorage system," IEEE Trans. Energy Convers., vol. 21, no. 1, pp.221–227, Mar. 2006. | [3] M. Jain, M. Daniele, and P. K. Jain, "A bidirectional dc-dc convertertopology for lowpower application," IEEE Trans. Power Electron., vol.15, no. 4, pp. 595–606, Jul. 2000. | [4] T. Kohama, M. Yamashima, and T. Nishimiya, "Operation-modecontrol of active-clamped bi-directional flyback converter as EDLCcharger and discharger," in Proc. Power Conversion Conf. (PCC),Osaka, Japan, 2002, vol. 3, pp. 1155–1159. | [5] A. D. Swingler and W. G. Dunford, "Development of a bi-directionaldc/dc converter for inverter/charger applications with considerationpaid to large signal operation and quasi-linear digital control," in Proc.IEEE Power Electronics Specialists Conf. (PESC), 2002, vol. 2, pp.961–966. | [6] F. Z. Peng, H. Li, G.-J. Su, and J. S. Lawler, "A new ZVS bi-directionaldc-dc converter for fuel cell and battery application," IEEE Trans.Power Electron., vol. 19, no. 1, pp. 54–65, Jan. 2004. | [7] L. Zhu, "A novel soft-commutating isolated boost full-bridgeZVS-PWM dc-dc converter for bi-directional high power applications,"IEEE Trans. Power Electron., vol. 21, no. 2, pp. 422–429, Mar.2006. | [8] L. Shi, L. Sun, D. Xu, and M. Chen, "Optimal design and ontrol of 5kWPWMplus phase-shift (PPS) control bidirectional dc-dc converter,"in Proc. IEEE Appl. Power Electron. Conf. Expo (APEC), Dallas, TX,Mar. 2006. | [9] Y. Hu, J. Tatler, and Z. Chen, "A bi-directional dc/dc power electronicconverter for an energy storage device in an autonomous powersystem," in Proc. Power Electron. Motion Cont. Conf. (IPEMC), 2004,vol. 1, pp. 171–176. | [10] H.-J. Chiu and L.-W.Lin, "A bidirectional dc-dc converter for fuel cellelectric vehicle driving system," IEEE Trans. Power Electron., vol. 21,no. 4, pp. 950–958, Jul. 2006. | [11] R. W. De Doncker, D. M. Divan, and M. H. Kheraluwala, "A threephasesoft-switched high-power density dc/dc converter for high-powerapplications," IEEE Trans. Ind. Appl., vol. 27, no. 1, pp. 63–73, Jan./Feb. 1991. | [12] M. H. Kheraluwala, R. W. Gascoigne, D. M. Divan, and E. D. Baumann,"Performance characterization of a high-power dual activebridge dc-to-dc converter," IEEE Trans. Ind. Appl., vol. 28, no. 6, pp.1294–1301, Nov./Dec. 1992. | [13] S. Inoue and H. Akagi, "A bidirectional isolated dc-dc converter as acore circuit of the next-generation medium-voltage power conversionsystem," IEEE Trans. Power Electron., vol. 22, no. 2, pp. 535–542,Mar. 2007. | [14] M. Pavlovsky, S. W. H. de Haan, and J. A. Ferreira, "Concept of 50kW DC/DC converter based on ZVS, quasi-ZCS topology and integratedthermal and electromagnetic design," in Proc. Eur. Conf. powerElectronics Applications (EPE), 2005. | [15] J. L. Duarte, M. Hendrix, and M. G. Simões, "Three-port bidirectionalconverter for hybrid fuel cell systems," IEEE Trans. Power Electron.,vol. 22, no. 2, pp. 480–487, Mar. 2007. | [16] W. A. Roshen, "A practical, accurate and very general core loss modelfor nonsinusoidal waveforms," IEEE Trans. Power Electron., vol. 22,no. 1, pp. 30–40, Jan. 2007. | [17] S. Inoue and H. Akagi, "Loss analysis of a bi-directional isolated dc/dcconverter," in Proc. Int. Power Electron.Conf. (IPEC), 2005. | [18] N. Mohan, T. M. Undeland, and W. P. Robbins, Power Electronics,Converters, Applications and Design, 3rd ed. New York: Wiley,2003, p. 342.ama, Japan.